FORTE satellite observations of very narrow radiofrequency pulses associated with the initiation of negative cloud-to-ground lightning strokes

Abram R. Jacobson (corresponding author)
ajacobson@lanl.gov
tel(505)667-9656 fax(505)665-7395
Space and Atmospheric Sciences Group
Mail Stop D466
Los Alamos National Laboratory
Los Alamos, New Mexico 87545

& Xuan-Min Shao
Space and Atmospheric Sciences Group
Mail Stop D466
Los Alamos National Laboratory
Los Alamos, New Mexico 87545

To be submitted to Journal of Geophysical Research (Atmospheres)

Los Alamos National Laboratory report LA-UR-01-01-6320

Abstract

The FORTE satellite's radiofreqency receiver/recorder system has been used to study extremely narrow (~100 ns width) radiofrequency pulses accompanying the initiation of negative cloud-to-ground strokes. These pulses have been observed from the ground for over two decades. The FORTE space-based observations are substantially consistent with the prior ground-based results, at least in regard to pulsewidth, distance-scaled pulse amplitude, and the pulses' basic association with negative cloud-to-ground strokes, relative to either positive cloud-to-ground or intracloud strokes. New results from the FORTE observations include (a) information on the radiation pattern (versus elevation angle), and (b) the tendency of the underlying fast-pulse radiation process to occur preferentially in marine, rather than dry-land, locations. These two new results were not accessible to ground-based measurements, which do not sample other elevation angles than zero, and whose signal distortion with over-land propagation paths (at zero elevation angle) tends to confuse the issue of the (land versus sea) location affinity of the pulse source itself. The narrow radiofrequency pulse that accompanies negative cloud-to-

ground strokes provides a useful identifier, in the satellite's radiofrequency datastream, of the occurence of this particular kind of stroke.

1. Introduction and Background

Among radio-frequency (RF) emissions from lightning, one of the most unique signals is also one of the most elusive to observe: A discrete, very narrow (~100 nanoseconds width) pulse accompanying the initiation of negative cloud-to-ground (-CG) strokes. This pulse differs in some key ways from most lightning RF signals and offers a potentially useful signature in remote sensing and characterization of lightning using high-frequency (HF; 3-30 MHz) and very-high-frequency (VHF; 30-300 MHz) spectral ranges. The HF band is amenable to ground-based, ionospherically reflected (over-the-horizon) remote sensing, while the VHF band is suitable for space-based monitoring (since signals at these frequencies penetrate the ionosphere).

During two decades of ground-based measurements, workers in this field have converged on a consistent picture of the basic characteristics of the RF pulse accompanying -CG initiation. Weidman and Krider [1980] employed a wideband, fast-response (instrumental risetime < 5 ns) transient recorder to collect vertical dE/dt signals in coastal western

Florida. Their site was chosen to exploit cases in which the signal path (from the stroke to the sensor) was mostly over seawater, so that the signal had experienced the least propagation distortion from a lossy (i.e., imperfect electrical conductivity) ground plane. Based on a selected set of >100 -CG stroke-initiation events, Weidman and Krider found a mean 10-90% risetime (of the integral of dE/dt) to be 90 ns.

The differential effect of seawater versus land propagation paths can be severe, owing to the several-order-of-magnitude enhancement of salt-water electrical conductivity relative to that of land materials. Cooray and Ming [1994] have reviewed methods of modeling ground-loss distortion/attenuation and have presented their own comprehensive calculations of spectral attenuation over a variety of land, sea, and combined land/sea paths. Their results make clear that several-km or longer propagation paths over land will sufficiently distort broadband radiated vertical electric field signals that pulsewidths on the order of 100 ns cannot be observed under those conditions. Similarly, they show that propagation paths of several tens of km over calm seawater will still preserve such transient features.

Levine *et al* [1989] studied the behavior of wideband dE/dt signals from both natural and triggered -CG subsequent strokes. Their site on the eastern Florida coastline allowed them to focus on signals whose propagation paths were entirely over seawater. Levine *et*

al found that the pulsewidths were substantially similar for both natural and triggered strokes' fast transients. In order to better discriminate against the effects of an underlying slow feature, they used the full width at half maximum (FWHM) of the fast dE/dt pulse, rather than the 10-90% risetime (of the integral of the fast dE/dt). This appears to have resulted in less scatter in the estimate of the pulsewidth, whose means were 78 ns for natural subsequent strokes and 61 ns for triggered strokes.

Willet *et al* [1990] performed careful spectral estimates of recorded waveforms for several classes of fast RF lightning signals, again for the case of propagation almost exlusively over seawater. They included electromagnetic impulses from both first and subsequent -CG return strokes, from three species of leaders, and from certain intracloud discharges. They found there was substantial similarity in spectral shape in the range 200 kHz- 20 MHz for all kinds of signals, but that the pulses from -CG stroke initiation were somewhat stronger.

Leteinturier *et al* [1991] performed close-in measurements of current I and of current derivative dI/dt at an instrumented triggered-lightning facility in Florida. For a subset of 56 strokes, they found that the dI/dt fast transient had a mean FWHM of 74 ns. This ground-truth characterization indicates that the remote measurements of fast dE/dt transients with sea-water propagation paths were indicative of the true widths of the

radiation source process. Comparable dE/dt widths have been more recently confirmed in careful multi-distance (10, 14, and 30 m) close-in measurements on triggered lightning by Uman *et al* [2000]. We stress however, that the physics of stroke initiation in the context of triggered lightning may not be entirely applicable to the initiation pulses in natural -CG strokes.

Krider *et al* [1996] further treated remote measurements of dE/dt for 63 -CG first return strokes at 35-km range over seawater. They found that the mean measured dE/dt FWHM of 100 ns is consistent with a true value of 75 ns corrected for the propagation spectral distortion over the seawater path. Willet *et al* [1998] presented a study of FWHM of the fast-pulse time-series data for the same strokes that had produced the spectra [*Willett et al.*, 1990], and found the FWHM of these marine -CG fast pulses to have a mean of 64 ns.

By contrast, Heidler and Hopf [1998] studied continental -CG strokes with an over-land propagation path and measured dE/dt FWHM values on the order of half a microsecond or more, but with much scatter (also on the order of half a microsecond). Interestingly, they showed that at least the wide scatter in these widths *could not be accounted for by propagation effects*. In response to this finding, Willet *et al* [1998] speculated that this

may be evidence for a real broadening, at the source, of the timescale for the -CG stroke-initiation transient on land relative to sea. That issue is as yet unresolved.

Willett and Krider [2000] have recently published a useful review and synthesis of several pulse-shape and pulse-width issues.

The narrow (FWHM < 100 ns) dE/dt transient characterizing -CG initiation over sea might allow observations of lightning with a satellite-based RF pulse recorder to recognize the occurrence of this category of lightning stroke, via the RF pulse characteristics gleaned over the past two decades from ground-based measurement. However, Willet *et al* [1990] and Willett and Krider [2000] show that FWHM < 100 ns is not unique to these -CG initiation transients. Rather, stepped-leader pulses, dart-stepped-leader pulses, and certain ("characteristic") intracloud pulses also share the narrow width with -CG initiation transients. Therefore, in order for a satellite-based RF transient recorder to reliably recognize -CG transients, more discriminants than FWHM must be available.

At least in the case of stepped-leader and dart-stepped-leader RF pulses, and in the case of repetitive intracloud pulses, pulsed RF signals from leaders should be easily discriminable from -CG initiation pulses on the basis of their repetition cadence. This is

because stepped-leader pulses for negative breakdown leaders necessarily occur in pulsetrains, due to the innate relaxation-oscillation nature of the negative discharge. See, for example, the wealth of original data on experiments on negative discharges in long (up to 10 m) air gaps [*Renardieres*, 1981]; see also modeling applications of this work and a useful synthesis of its theoretical description, eg. Mazur *et al* [2000]. Observed leader pulses are almost always grouped into pulse-trains. For example, Krider *et al* [1975, note reversal of figure captions for Figures 3 and 4] studied repetitive Florida intracloud leader-step signals, and they noted typical per-pulse FWHM in the range 0.5-1.0 μs and typical interpulse separation in the range 2-15 μs. Similarly, Cooray and Lundquist [*Cooray and Lundquist*, 1985] amassed statistics of observed stepped-leader inter-pulse time separations which confirmed those of Krider *et al* but were based on tropical lightning in Sri Lanka. Proctor's [1981] classic characterization of lightning VHF signals summarizes the repetition rate of leader pulses as ranging from 10^3 to 10^5 pulses per second. Bondiou *et al* [1990, see their Figure 12] show very clearly that virtually all lightning VHF emissions contributing to interferometer maps of lightning emitters are part of more-or-less irregular pulsetrains, with interpulse spacing > 2 μs for (slow-propagating) stepped leaders and < 1 μs for (faster-propagating) recoil streamers. The authors infer that the elementary emission pulse in such pulsetrains, based on observations in laboratory discharges, should have a risetime on the order of 5 ns. Such

individually narrow, but copious pulsetrain emissions are very different from the essentially isolated monopulse associated with -CG stroke initiation, and it would not be easy to confuse these very different phenomena in a transient recording of sufficient length (say, >100 μs).

An event which can occur only once per stroke, such as the transient pulse associated with -CG stroke initiation, *a fortiori* can not be observed any more frequently than the controlling strokes occur- and this inter-stroke time is in the range of tens of milliseconds, and almost never less than a millisecond. Therefore, if a satellite-borne RF transient recorder sees a short RF pulse that lacks any similar neighbors within a millisecond, then we may legitimately doubt that the pulse is from a negative stepped leader, whether in-cloud or descending to ground.

The remaining species of RF pulse which might be difficult to distinguish from a pulse associated with -CG stroke initiation are solitary in-cloud discharges. This logically would include the extremely bright RF emissions noted by Le Vine [1980], Willett *et al* [1989], and Smith *et al* [1998], as well as Taylor's [1984] "minor flashes" which occur relatively high in the cloud and consist of solitary RF emissions without close neighbors either temporally or spatially. Fortunately, it is easy with a satellite RF transient recorder to discriminate between emissions on the ground (such as the narrow transient associated

with -CG stroke initiation) and emissions at height: Emissions at the ground reach the satellite by the direct path. Emissions at height reach the satellite not only by the direct path, but also by the longer path consisting of a ray from the emission to the ground, then a specular reflection at the ground, and finally a ray from the ground to the satellite. These pulse pairs were first noted by Holden *et al* [1995]. The basic validity of the reflection model was further established by Massey [1995; 1998a], and Jacobson *et al* [1999]. For the satellite near the zenith, the inter-pulse separation (between the pulses arriving on the shorter and longer paths) is $\delta t=2h/c$, where h is the emitter's height above ground and c is the speed of light. Considering a pulse of 100-ns FWHM, we therefore could resolve its height down to ~15 m. At satellite zenith angles greater than zero, the resolution decreases in a known way [*Jacobson et al.*, 1999], but there never is a difficulty in telling the difference between an emitter on the ground and an intracloud emitter. In conclusion, then, the outlook is favorable for satellite RF transient recordings of 100-ns pulses associated with -CG stroke initiation to correctly identify their lightning setting, and to avoid confusing the narrow pulse with other known lightning phenomena.

In the remainder of this paper, following a brief review of the RF transient-recorder capabilities of the FORTE satellite, we will present the basic characteristics of FORTE recordings of 100-ns-FWHM pulses associated with -CG stroke initiation. A follow-on

paper will present evidence for the emission beam-lobe of the presumably vertical current channel responsible for these pulses.

2. RF transient recording by the FORTE satellite

The FORTE satellite has observed lightning continually since its launch on 29 August 1997. FORTE is in a 70° inclination, circular low-Earth orbit and makes several passes per day over lightning-prone tropical regions, notably South America, Africa, and SE Asia/ Indonesia, as well as over the less lightning-prone midlatitudes. FORTE captures and stores discrete records of VHF lightning time series waveforms of the RF electric field, E. The radio-frequency receiver whose data are used in much of this study comprises dual, simultaneous 50-Megasample-per-second passbands, each analog-filtered to 22-MHz bandwidth. In the data to follow, we always operated the RF payload with at least one of the 22-MHz channels placed in the range 26-48 MHz, with a nominal 38-MHz center ("low band"). The performance of the FORTE rf payload, plus some of the initial characteristics of the lightning observations, have been described in detail elsewhere [*Jacobson et al.*, 1999], so only the most pertinent information is repeated here.

There are eight “trigger subbands” in each 22-MHz-wide receiver channel. Each 1-MHz-wide trigger subband has a noise-compensation option, so that the trigger threshhold is either set in absolute level or as dB *above a low-pass-filtered noise level* in that 1-MHz subband, i.e. as a “noise-riding threshold”. In this way the trigger system can in practice trigger on lightning signatures that would otherwise be overwhelmed by anthropogenic radio carriers appearing in the overall analog passband. In the data used here, we use noise-riding-threshhold triggering and require five (out of eight) 1-MHz subbands to trigger in correlation. We typically require the signal to rise at least 14 - 20 dB (depending on the program and the intended class of lightning signals) above the noise background in each 1-MHz subband contributor to the “5-out-of-8” logical-OR condition. These contributing channels must arrive within a coincidence time of 162 μs of each other. This coincidence window allows for arrival of different frequencies from the same event, in the presence of ionospheric dispersion of the pulse. (“Ionospheric dispersion” is the effect of the ionospheric plasma's imposing a group delay on the rf pulse, with the delay varying roughly as $1/f^2$.)

The ionospheric $1/f^2$ dispersion causes the lowest frequencies to arrive latest, as in a “chirp”. For this reason the VHF signals which have been transmitted through the ionosphere are referred to as “chirped” signals. Similarly, the signal-processing step of

removing the dispersion is called “dechirping”. We perform dechirping on all archived VHF signals from FORTE.

Both 22-MHz-bandwidth channels are connected to different linear polarizations of a two-polarization log-periodic antenna. The antenna is mounted on a boom that is directed toward the satellite nadir, usually within a few degrees or less of true pointing. The antenna is designed to place an approximate minimum (throughout the VHF spectrum) on the limb of the Earth as seen from FORTE, and a lobe maximum at nadir. The limb is a circle of arc-diameter 6,400 km on the surface of the Earth.

The Data Acquisition System (DAS) contains enough memory for up to 0.8 seconds (cumulative) of 12-bit data simultaneously from the two 22-MHz channels. Each record is triggered (see above) and has adjustable pre/post-trigger ratio. We typically use 400-μs records with 100 μs of pretrigger samples and 300 μs of posttrigger samples. There is typically room in DAS memory for ~2000 such events between downloads. Since we can have up to several downloads per day, in principle we can acquire up to ~10000 such events per day. Usually, however, operations constraints and limited availability of suitable lightning storms near the FORTE track limit us to less than this theoretical maximum.

The DAS is capable of beginning a new record 162 μs after the end of the previous record, so that FORTE records can effectively mosaic-together to form a quasi-continuous registation of VHF signatures arriving one-upon-the-other within a flash. We find in practice that the registration of records is not impeded by the necessary DAS dead time between records, but rather is spaced wider apart by the natural cadence of the emission process itself.

The configuration described above was followed between launch (August 1997) and December 1999. During this ~ 28-month campaign, FORTE gathered over 3-million data records, the vast majority of which were due to VHF emissions from lightning. More recently (starting in January 2000) we have used a wider-band (85-MHz analog bandwidth), whose initial results are described by Light *et al* [*Light et al.*, 2001]. At the time of this writing (Autumn 2001) the total cumulative event count for the FORTE data archive exceeds 4 million.

3. Observed properties of FORTE-recorded signals associated with -CG stroke initiation

3.1 FORTE/NLDN event coincidences

The most important tool in making any association of FORTE-recorded signals with stroke characteristics has been comparison with contemporaneous data from National Lightning Detection Network (NLDN), in a collaboration between the FORTE team and Global Atmospherics, Inc, the array's developer/owner/operator. The NLDN is a system of low-frequency (LF; 30-300 kHz) and very-low-frequency (VLF; 3-30 kHz) electromagnetic sensors in an array covering lightning throughout the continental United States [*Cummins et al.*, 1998; *Idone et al.*, 1998a; *Idone et al.*, 1998b]. The NLDN is comprised of 59 LPATS-III Time-of-Arrival (TOA) sensors and 47 IMPACT sensors that provide both TOA and direction-finding information. The median location accuracy provided by the NLDN is 500 meters, and the estimated flash detection efficiency varies between 80 and 90 percent, for peak currents greater then 5 kA [*Cummins et al.*, 1998; *Idone et al.*, 1998a; *Idone et al.*, 1998b].

The NLDN sensors are responsive to radiation field signals in the LF and VLF frequency ranges, and are thereby sensitive to ground-wave lightning return-stroke fields over a

spatial range of about 30 to 650 km. They are also responsive to lightning-produced VLF fields that have been reflected by the ionosphere, and to a subset of fields produced by cloud discharges that emit significant energy in the LF frequency range. The IMPACT sensors are designed to reject many of these cloud discharges and "reflected" signals, based on waveform criteria, but the LPATS-III sensors accept a broader range of waveshapes.

The standard NLDN lighting data are carefully quality controlled and limited to minimize mis-located "outlier" events, employing specific criteria [*Cummins et al.*, 1998]. For the purposes of this study, we reprocessed the raw sensor from the LPATS-III sensors employing relaxed criteria, in order to maximize the detection of both cloud discharges and distant CG discharges. Specifically, "unverified" locations produced by three LPATS-III (TOA) sensors were accepted, no maximum limit was set for the distance between a sensor and the discharge location, and a number of waveform-consistency criteria were relaxed to accommodate ionospherically propagated signals. The resulting dataset therefore included some very distant CG lighting discharges (sferics), occurring several thousand km outside the network, as well as very energetic cloud discharges occurring within or near the network. Given the relaxed criteria, the dataset also included numerous outliers. This did not pose a problem in the current study, since the lighting data was time-correlated with FORTE events with 10-μs resolution.

The located lightning discharges were classified as follows. Events for which all contributing sensors reported a narrow pulse-width, identified by a peak-to-zero time of less than 10 μs, were identified as cloud discharges. All other discharges were identified as cloud-to-ground. For those events in which the closest reporting sensor was more than 625 km from the calculated location, the estimated signal strength (peak current) was set to zero. This assignment reflects the uncertainty in the source strength when the ground wave becomes smaller than the ionospheric reflection.

The FORTE/NLDN joint campaign has been done in three segments: April-September 1998, May-October 1999, and April-September 2001. This article will deal with data from the first two campaign segments. Those two segments allowed us to gather ~25,000 reliable coincidences between FORTE VHF events and NLDN strokes. The method for establishing these coincidences, and for characterizing their reliability, is explained elsewhere [*Jacobson et al.*, 2000]. The 25,000 coincidences are corrupted by approximately 2% false coincidences; that is, the 25,000 coincidences are 98% reliable.

Plate 1(a) shows the geographical location of the ~25,000 NLDN strokes to which at least one FORTE RF recorded event is associated, within a time separation (corrected to the stroke location) of ± 300 μs. The green points are -CG strokes, the blue points are +CG

strokes, the black points are strokes that cannot be reliably characterized (being farther than 625 km from the nearest participating NLDN sensor station), and the red points are intracloud (IC) strokes. Noteworthy is the large number of -CG strokes (green) over the Gulf Stream.

Plate 1: (a) Map of ~25,000 NLDN stroke locations that are accompanied by closely coincident FORTE VHF events. The stroke type is marked in color: green= -CG, blue=+CG, red=IC, black=uncharacterized type (due to the nearest participating NLDN station being >625 km from the stroke.) (b) Similar, but for the ~2400 FORTE VHF events meeting the automatic selection criteria to qualify as extremely narrow pulses.

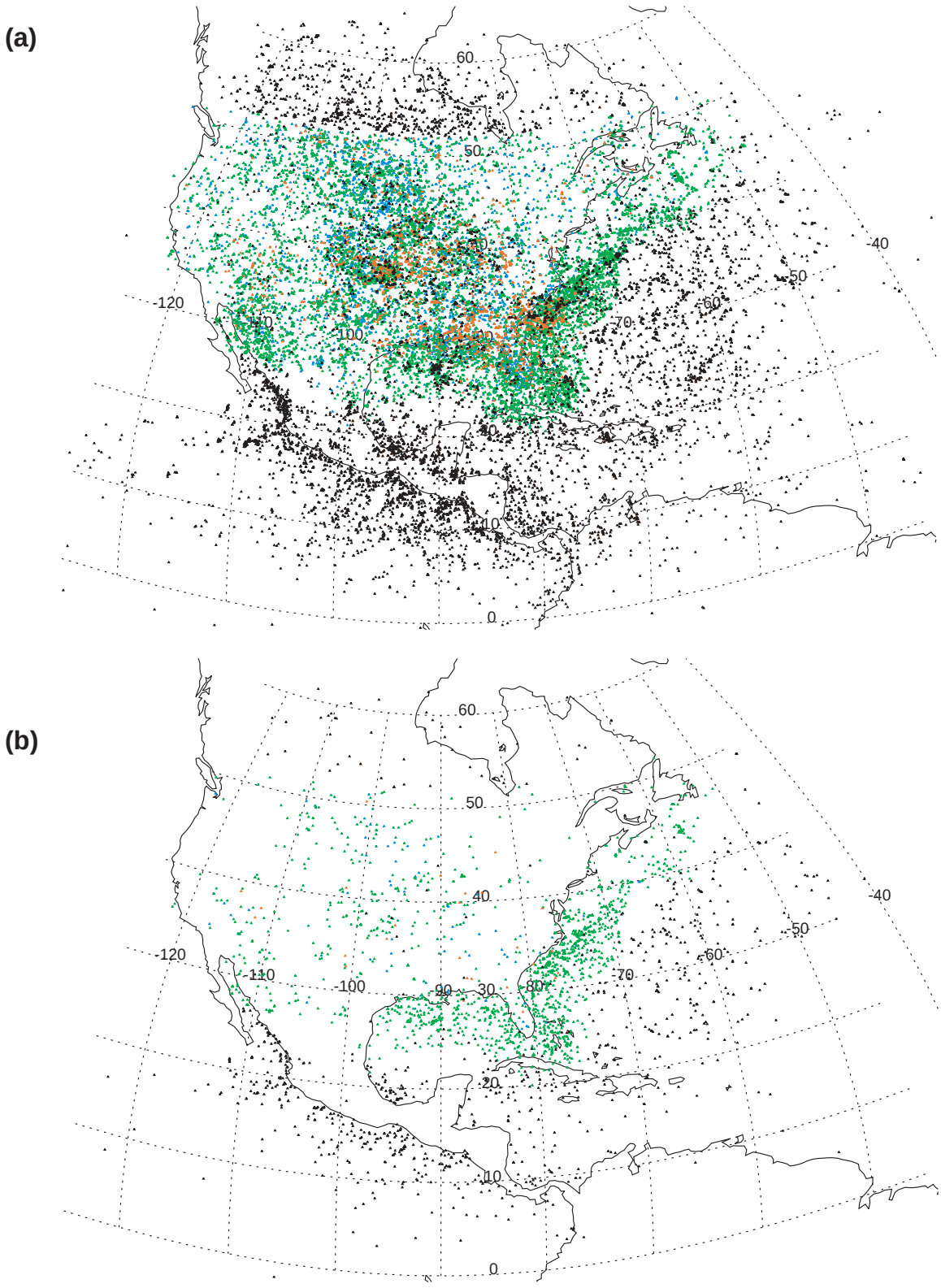
(a)
60
50
40
-120
-110
-100
-90
-80
-70
-60
-50
-40
30
20
10
0
(b)
60
50
40
-120
-110
-100
-90
-80
-70
-60
-50
-40
30
20
10
0

3.2 Impulse response for FORTE transionospheric pulsewidth measurements

A remarkable feature of RF pulses accompanying -CG stroke intiation is their narrow pulsewidth (< 100 ns FWHM according to ground-based wideband measurements.) The question arises, can a signal from this source, captured by a satellite-borne RF transient recorder (such as FORTE), be expected to preserve the FWHM < 100 ns? There are two factors to consider:

(a) An advantage of a satellite-borne RF sensor, relative to a ground-based recorder on dry land, is that the obliquely-upward raypath from the stroke-initiation source to the satellite minimizes the propagation path's proximity to the imperfect-conductor, lossy ground. This in turn minimizes the spectral distortion (selective attenuation of the signal's higher frequencies) and subsequent pulse-lengthening expected for a ground-based observer [*Cooray and Ming*, 1994].

(b) A disadvantage of a satellite-borne RF sensor is the dispersive group delay caused by the propagation through the ionosphere [*Jacobson et al.*, 1999; *Jacobson and Shao*, 2001; *Massey et al.*, 1998b; *Shao and Jacobson*, 2001]. To first order, there is a dependence of group delay versus frequency varying as N/f^2, where N is the path-integrated total electron content, in units of electrons/m^2. There are ray-bending effects that first appear to order $1/f^4$. In addition, the propagation modes in a magnetized plasma (like the ionosphere) are the "ordinary" and "extraordinary" modes, which are approximately circularly polarized (but of opposite sense), and whose differential group delays are

manifested as a time-splitting (varying as $1/f^3$) in the received signal [*Jacobson and Shao*, 2001; *Massey et al.*, 1998b] after it has propagated to the satellite through the ionosphere. Finally, there is the liklihood of random scintillations in both the phase and amplitude of the received signal, due to refraction of the RF wavefront in spatially random ionospheric electron-density irregularities. The deterministic dispersive effects (N/f^2 gross dispersion, raybending, and magnetic mode-splitting) in the received RF signal can often be compensated by painstaking analysis, but the random scintillations cause irremediable broadening and fading of the signal.

We have used a very high-power artificial emission source of negligible pulsewidth to characterize the impulse response of the transionospheric channel, in order to assess the cumulative effect of all the difficulties mentioned above. We use the Los Alamos Portable Pulser (LAPP) [*Massey et al.*, 1998b] to illuminate FORTE from the ground. The LAPP emitts a broadband VHF pulse, of FWHM < 20 ns, with a peak effective isotropic radiated power of several-hundred megawatts. Plate 2(a) shows a spectrogram of a LAPP signal recorded by FORTE, in the 26-51 MHz “low band”. Both the gross dispersion and the magnetic-mode time splitting are evident. The time/frequency pixel in this spectrogram has approximately a 1.3-μs time width, and it is advanced by steps of 1/16 of that width. Plate 2(b and c) shows zoomed spectrograms of the same signal, with dispersion correction optimized for the ordinary (Plate 2b) and extraordinary (Plate 2c)

modes separately. The signal has been bandpass-filtered prior to the zoomed spectrograms, in order to suppress the spectral region where the two modes are poorly resolved in time (f>47 MHz) and to suppress the region corrupted by a strong carrier interference (f<32 MHz). The time width of a pixel in the zoomed spectrograms is 0.3 μs; it is advanced by steps of 1/16 of that width.

Plate 2: Spectrograms for a LAPP pulse, to demonstrate the end-to-end system response of the combined effect of both the ionospheric propagation and FORTE receiver characteristics. (a) Raw, full-bandwidth data showing ionospheric dispersion and birefringent mode splitting. The time resolution is effectively 1.3-μs wide, and it is advanced by steps of 1/16 of that width. (b) Expanded view of signal after bandpass filtering and after dechirping, optimized for the ordinary mode. The time width of a pixel in this spectrogram is 0.3 μs; it is advanced by steps of 1/16 of that width. (c) Similar to (b), but for the extraordinary mode.

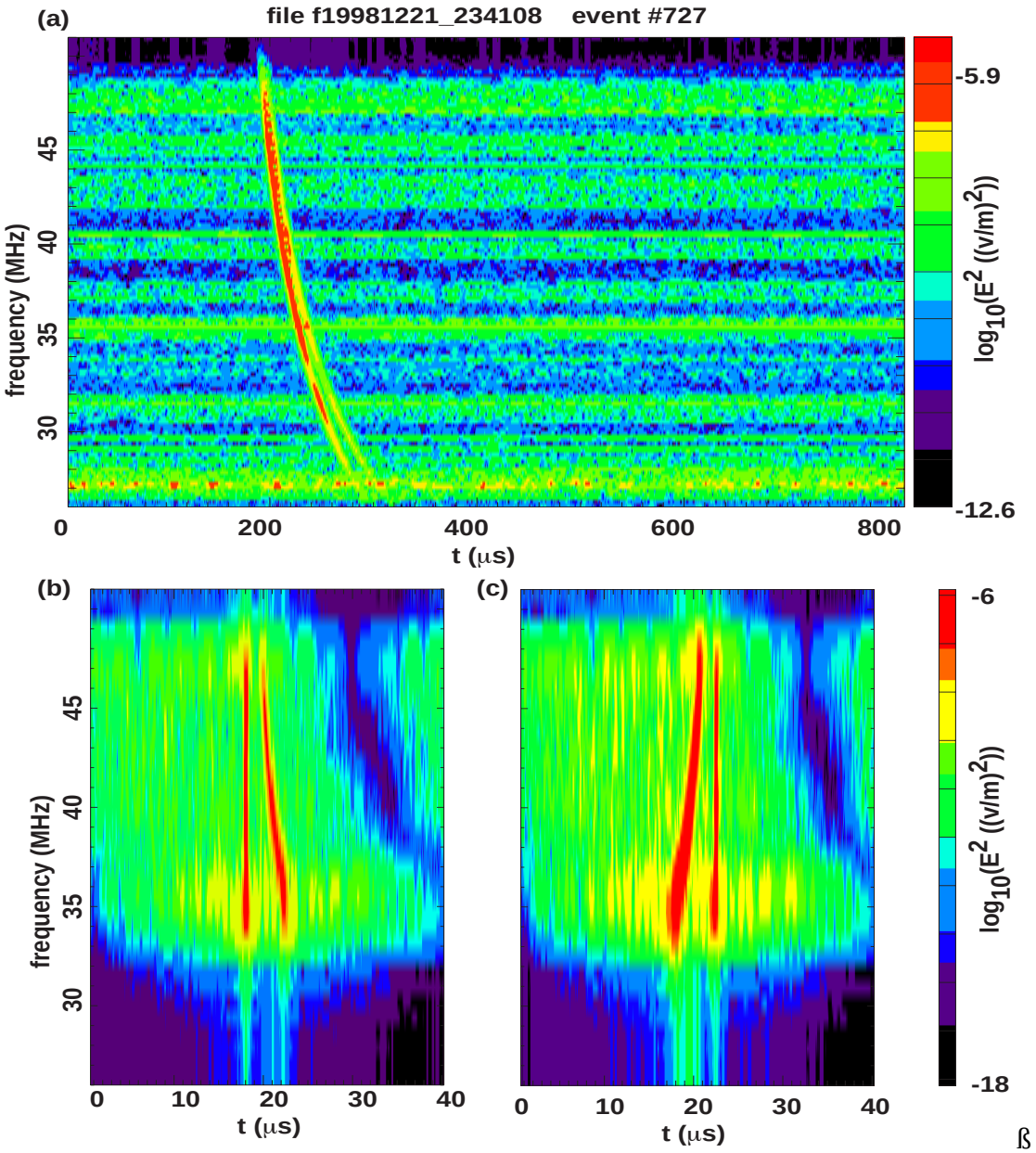

ß

Figure 1 shows the envelope of E^2 of the time-domain signal whose zoomed spectrograms are in Plate 2(b,c). (The envelope is actually the sum of the square of E plus the square of the Hilbert transform of E [*Massey et al.*, 1998b].) Figure 1(a) shows the ordinary mode, and Figure 1(b) shows the extraordinary mode. The envelopes have a FWHM on the order of 80-100 ns. This is quite typical of our experience with the LAPP pulse propagated through the midlatitude ionosphere. The same (midlatitude) ionospheric conditions apply to much of the data on lightning (see Plate 1a) treated in this study. The propagation paths for lightning data observed from FORTE in this study are largely free of either magnetic-equatorial or auroral scintillations, either of which could be much more pronounced than the scintillation condition seen here with the LAPP.

Figure 1: Envelope of E^2 of the time-domain signal for the LAPP pulse of Plate 2. (a) With the signal dechirped for ordinary mode. (b) With the signal dechirped for extraordinary mode.

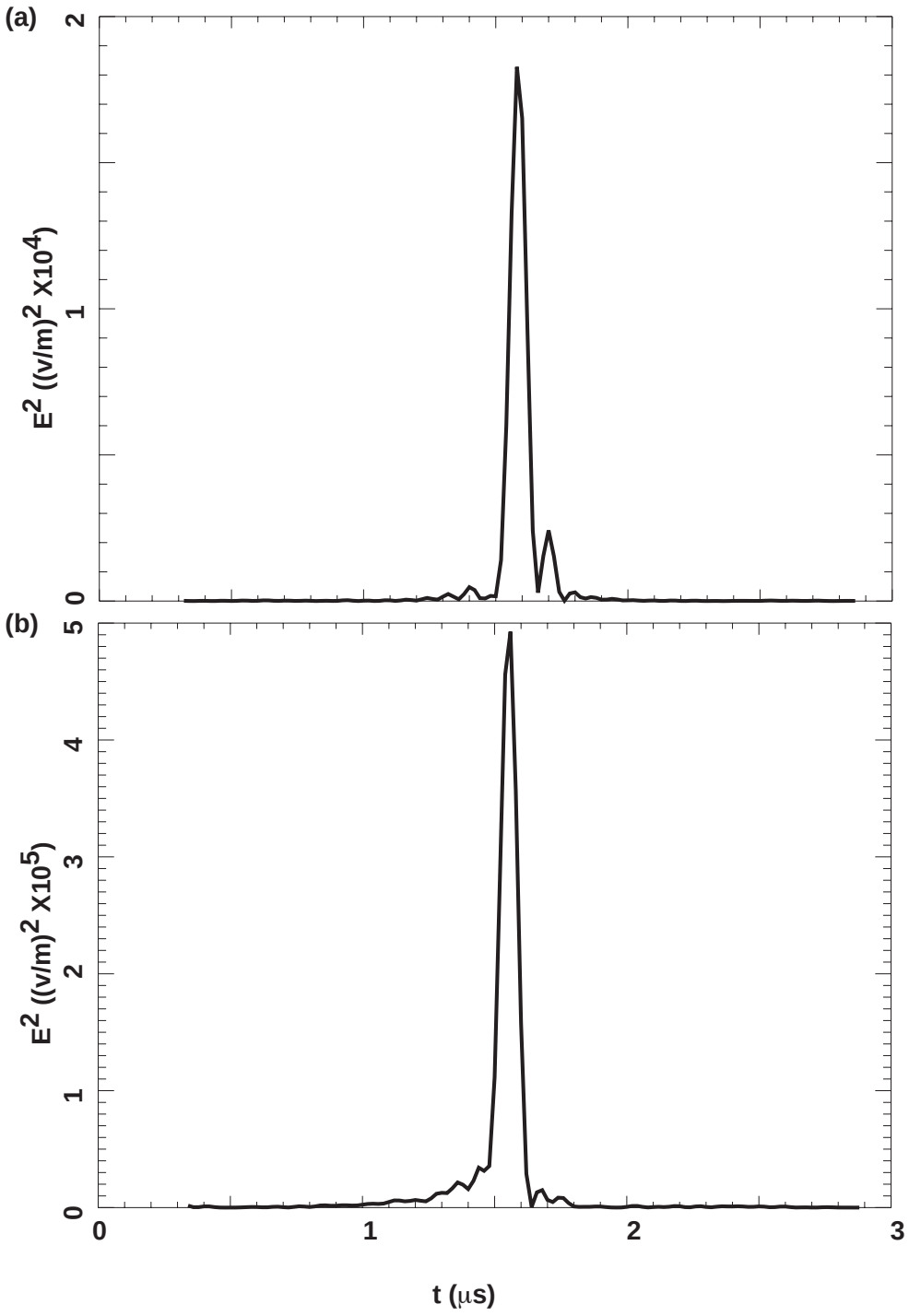

Notwithstanding the relatively benign midlatitude-ionosphere conditions here, it should be pointed out the the end-to-end system broadens the LAPP pulse more than can be accounted-for by sampling theory. Our bandpass width (see the zoomed spectrograms in Plate 2b,c) is about 15 MHz. Therefore we are limited by bandwidth alone to a point-impulse-response on the order of 60-70 ns, which is shorter than our received-pulse FWHM of 80-100 ns. We must attribute the excess broadening (~30 ns) to some combination of (a) imperfect dispersion compensation and (b) random scintillations. That our end-to-end (including propagation effects) FWHM is 80-100 ns implies that FORTE is not in a position to measure as short a pulsewidth as could some of the broadband ground-based measurements made previously (see Section 1 above).

3.3 Determination of width of FORTE-recorded -CG stroke-initiation pulse

We now apply exactly the same pulsewidth-determination methodology to a pulse from a -CG stroke initiation. This is shown in Plate 3. The overall spectrogram (Plate 3a) is 800 μs long, twice as long as the LAPP recording shown in Plate 2(a). The narrow VHF pulse occurs between 200 and 240 μs on in this spectrogram. The pulse is preceded by some leader activity. We speculate that the broader signal later in the record (600-700 μs) is similar to post-return-stroke radiation seen by VHF interferometry [*Shao et al.*, 1995, see e.g. their Figure 11(a)]. The zoomed spectrograms (Plate 3b,c) of the narrow pulse show

that we have used a more restrictive passband, necessitated in this case by the unresolved mode splitting in the upper part of the spectrum. The envelopes of E^2 are shown in Figure 2. Their FWHMs are close to 100 ns, slightly wider than the end-to-end system response as revealed by the LAPP data. Therefore, we can claim only that the FWHM must be less than 100 ns, but we cannot reliably specify the width with finer resolution. Fortunately, this pulse (even with unknown ionospheric broadening) is still easily recognizable and appears unlike most other FORTE-recorded lightning signals.

Plate 3: Similar to Plate 2, but for a narrow pulse associated with a -CG stroke.

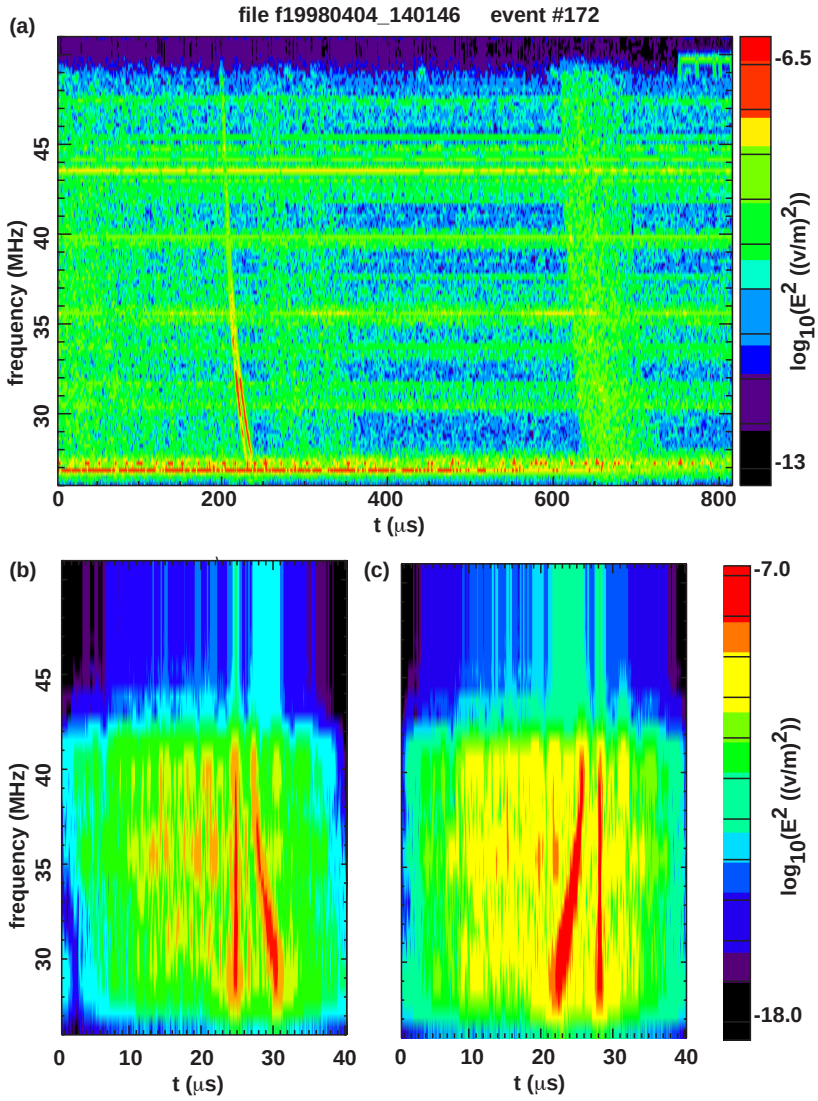

Figure 2: Similar to Figure 1, but for the narrow pulse associated with a –CG stroke.

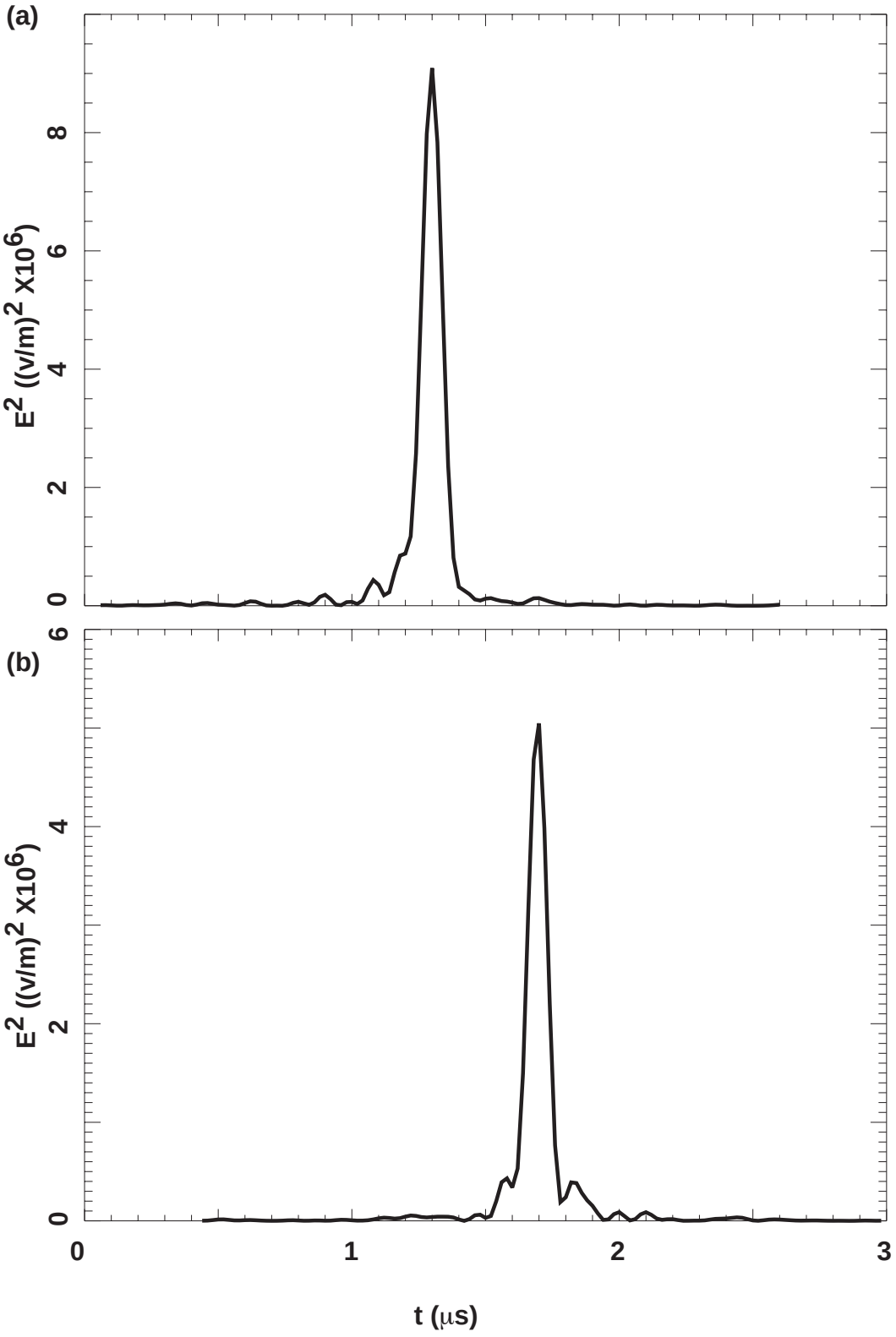

3.4 Polarization of signal from -CG stroke initiation

Most RF signals from lightning seen by FORTE are randomly polarized. This is consistent with the picture of there being an ensemble of discharges which overlap in time and occur at the multiple corona tips in negative-polarity air breakdown [*Bondiou et al.*, 1990; *Renardieres*, 1981]. Their orientations are somewhat random, their timings are not synchronized, and their net far-field radiation is therefore both incoherent and of randomly fluctuating polarization ("unpolarized").

However, some RF pulses observed by FORTE are linearly polarized, in a manner that can be recognized as alternately constructive and destructive ("fading") interference between the two propagation modes [*Jacobson and Shao*, 2001; *Massey et al.*, 1998b]. The amplitude modulation is at a frequency $\delta f = 2 f_{ce} \cos(\beta)$, where f_{ce} is the electron gyrofrequency (in the ionospheric layer), and β is the angle between the wavevector and the geomagnetic field. For example, most of the narrow RF pulses associated with -CG stroke initiation are linearly polarized according to this observable. A follow-on paper will examine this more systematically, but for the present we note that most of these pulses exhibit the inter-mode interference which indicates substantial linear polarization. The pulse treated in Plate 3 and Figure 2 is no exception. When the ionospheric dispersion is retained, as in Plate 3(a), there is pronounced inter-mode amplitude beating.

Figure 3(a) shows the envelope of E^2 averaged over ±100 ns , during 60 μs centered on the pulse. The amplitude modulation is almost 80% peak-to-peak, so the implied linear polarization is significant. Figure 3(b) shows the spectrum of the E^2 modulation, and this is peaked at 1.92 MHz, corresponding to $f_{ce}\cos(\beta) = 0.96$ MHz.

Figure 3: Birefringent mode beating for the raw data of Plate 3 and Figure 2. (a) Envelope of E^2 averaged over ±100 ns , during 60 μs centered on the pulse. (b) Fading spectrum from the envelope above.

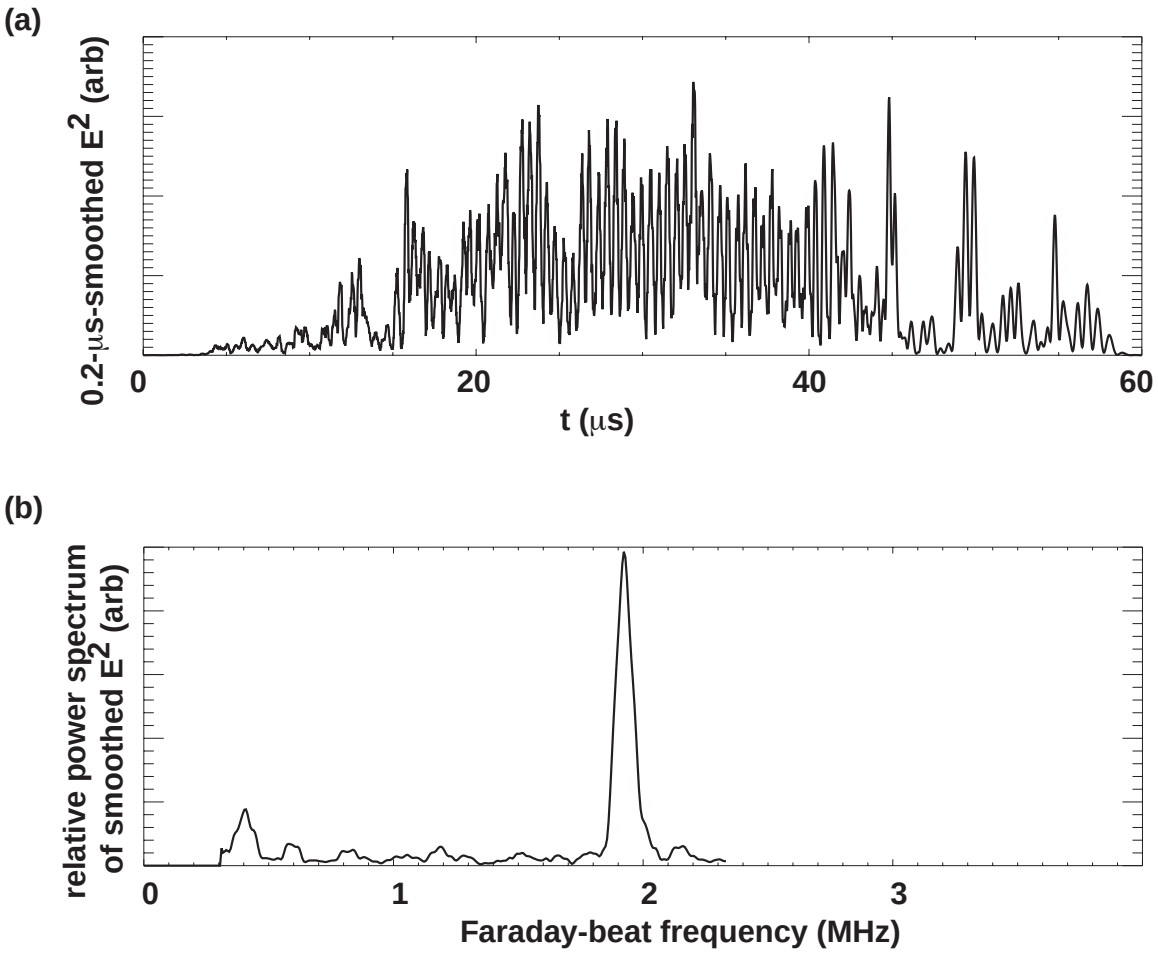

3.5 Association with stroke onset

The ground-based measurements (see Section 1 above) indicate that the narrow VHF pulses observed by FORTE around the time of -CG stroke initiation should occur in precise coincidence with stroke initiation. In our observations, the relationship is less precise, for instrumental reasons. The FORTE-observed narrow pulse described above systematically occurs within 10 μs of -CG stroke initiation, after correction for all known propagation delays to the source [*Jacobson et al.*, 2000]. The 10-μs uncertainty derives from the instrumental scatter in FORTE time-stamping and in our knowledge of FORTE satellite location. Spatially, this is equivalent to a 3-km uncertainty in satellite location. The 10-μs uncertainty appears as a spread of the histogram of times of FORTE and NLDN events, all times being referred to the stroke location [*Jacobson et al.*, 2000]. The NLDN possesses 0.5 km spatial-location accuracy for most -CG strokes occuring over land within the continental United States. The marine events may have more blurred NLDN geolocations, due to their being at the margin of NLDN array coverage. However, the near-shore -CG strokes accompanied by FORTE narrow VHF pulses show just as big a timing spread (of FORTE timestamps relative to NLDN) than do the further-offshore -CG strokes. Therefore we are inclined to attribute the major portion of the 10-μs uncertainty (in the timing of the narrow VHF pulses relative to NLDN stroke timing) to FORTE location and timestamping errors.

The pulses we see in association with stroke onset show a dramatic enhancement of VHF power, relative to the preceding period of stepped-leader-generated VHF. To show this, we use a FORTE VHF record of VHF signals associated with both leader and stroke-initiation processes during a marine -CG located off the east coast of Florida. Figure 4 shows the post-dechirping envelope of E^2 averaged over 0.4 μs, during a non-typical record in which the FORTE analog-to-digital recording extends over 8 millisec, so that the leader development can be seen as well as the stroke-initiation transient. Figure 4(a) shows the entire 8 millisec, while Figure 4(b) is an enlargement of the final 2.5 millisec; in each case the vertical axis is logarithmic. The regular pulses in Figure 4(a) are due to a communications signal, not the leader activity. The period between 4 millisec and the stroke, i.e. the final 4 millisec, show enhanced and growing leader noise. The stroke-initiation enhancement of VHF power in the final narrow peak is by more than an order-of-magnitude. This behavior is typical of the relationship of the FORTE-observed stroke-initiation transient to the prior leader-associated VHF. We note that the enhancement seen here is visible due to the rather precise dechirping of the time-domain signal E(t) prior to displaying the envelope of E^2 averaged over 0.4 μs. Had the dechirping not been done, or had it been done imprecisely, the final VHF pulse would have been far less visible relative to the leader noise. That is because the leader noise, being quasi-continuous, does not have the same amplitude enhancement with precise

dechirping as does an isolated, narrow pulse. In general, we find that satellite-recorded waveforms of these narrow VHF pulses are most recognizable, and most separable from the background of more continual lightning emissions, after the dechirping is first accomplished with precision. The narrow VHF pulses are often overlooked when the data is viewed while still “raw” and yet to be dechirped.

Figure 4: An unusual FORTE recording of a narrow pulse, in which it occurs at the end of an 8-millisec record. The regular pulses are from a communication carrier. (a) Envelope of E^2 for the entire record. (b) Envelope of E^2 during the final 2.5 millisec.

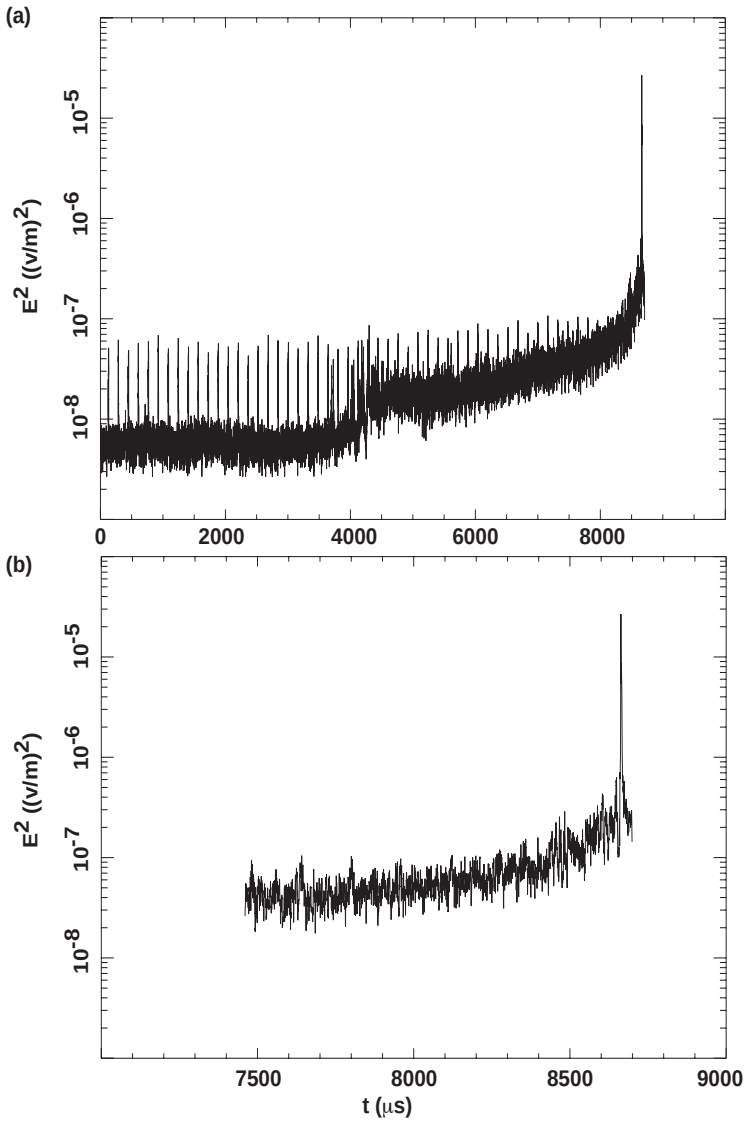

3.6 Statistical properties of VHF pulses associated with -CG stroke initiation

We have constructed a narrow-pulse selection algorithm to operate automatically, for computer selection of the narrow VHF pulses from amongst the 25,000 FORTE VHF records coincident with NLDN-detected strokes. The algorithm dechirps the data and searches for narrow (FWHM < 200 ns) pulses of either the ordinary or extraordinary mode. The geographic locations of the 25,000 coincident events' corresponding strokes is shown in Plate 1(a). The computer-selected narrow pulses are a subset of these and are shown in Plate 1(b). The algorithm finds only ~2400 narrow (<200 ns FWHM) pulses (less than 10% of total). Of these, the points in Plate 1(b) contain approximately 1400 which are green (i.e., -CG strokes). Only a few are blue (+CG strokes) or red (IC strokes). The rest are black (i.e., located further than 625 km from the nearest participating NLDN sensor, and hence not reliably characterizable as to stroke type.) Spot checks by eye of the computer algorithm reveal that its false alarm rate may be as high as 20%. That is, the selected 2400 narrow events may include to 20% which are revealed by visual inspection not to be narrow, singular pulses.

An obvious inference from comparison of Plate 1(a) and Plate 1(b) is that the narrow VHF pulses observed by FORTE are much more likely to be associated with -CG strokes than with either +CG strokes or IC strokes. This is completely consistent with the ground-based observations reviewed in Section 1.

Notwithstanding the selection algorithm's shortcomings, the 2400 selected pulses show a strong affinity to occur over seawater. Let us make this quantitative, by comparing the ~10,000 -CG strokes (having coincident FORTE VHF events, but not necessarily narrow pulses) with the ~1400 -CG strokes selected to have coincident narrow VHF pulses seen by FORTE. Over land, the ratio of (-CG strokes with narrow VHF)/(-CG strokes associated with any VHF) is 3.7%. Over seawater, that ratio is 15.8%. Given the algorithm's estimated false-alarm rate on the order of 20%, these results are consistent with the hypothesis that -CG strokes associated with narrow VHF are *exclusively over seawater*. However, this extreme statement remains conjectural, given the selection algorithm's shortcomings, and for the time being we can say only that the narrow VHF pulses are more likely over sea than over land.

The NLDN stroke data provide a report on each stroke in a flash, as long as the stroke exceeds the detection criteria already reviewed [*Cummins et al.*, 1998]. Thus, for -CG flashes, we can examine the strokes (if there are any) in the same flash which contains a stroke accompanied by a FORTE-observed VHF event, and thereby infer the relative liklihood of FORTE observing a coincidence for subsequent strokes versus first strokes within the flash. Let us call a stroke that has a FORTE VHF event tightly coincident with it a "key stroke". Then the question we pose is, what is the time distribution of co-located

strokes relative to the key stroke? That is, what is the time distribution of the key stroke's same-flash neighbors? Figure 5 shows the probability of a same-flash neighbor stroke, relative to the key stroke, versus time difference. Negative times are for the neighbor stroke preceding the key stroke, while positive times are for the neighbor stroke following the key stroke. The solid curve is for all ~10,000 -CG strokes (see the green points in Plate 1a above), while the dashed curve is for the ~1400 -CG strokes associated with selected narrow VHF pulses (see the green points in Plate 1b above). The key event is not counted as a neighbor of itself, and thus the depletion of probability near zero time is just a reflection of the unliklihood of strokes occuring more closely to each other than .02 s or so. The vertical axis scale is in probability per 0.01-s bin of time separation.

Figure 5 gives two significant insights into the kind of -CG stroke that is accompanied by FORTE-observed narrow VHF pulses. First, these strokes are only half as likly to occur in flashes that contain more than one stroke. This is seen by the overall lower level of the dashed curve compared to the solid curve. Second, in cases where the flash contains more than one stroke, FORTE-observed narrow VHF pulses are equi-probable both late and early in the flash. These narrow VHF pulses are not confined to occur only in association with first strokes, and nor are they confined to occur only in association with subsequent strokes, when they occur in a flash that contains more than one stroke.

Figure 5: Observed probability of delay between a neighboring stroke and the "key stroke" (which is closely coincident with a FORTE VHF event), per 0.01-s bin. The solid curve is for all ~10,000 -CG strokes having FORTE coincidence. The dashed curve is for the subset of these in which the coincident FORTE VHF pulse meets automatically applied criteria for extreme narrowness (<200 ns). The key event is not allowed to be entered as a neighbor of itself in the distribution.

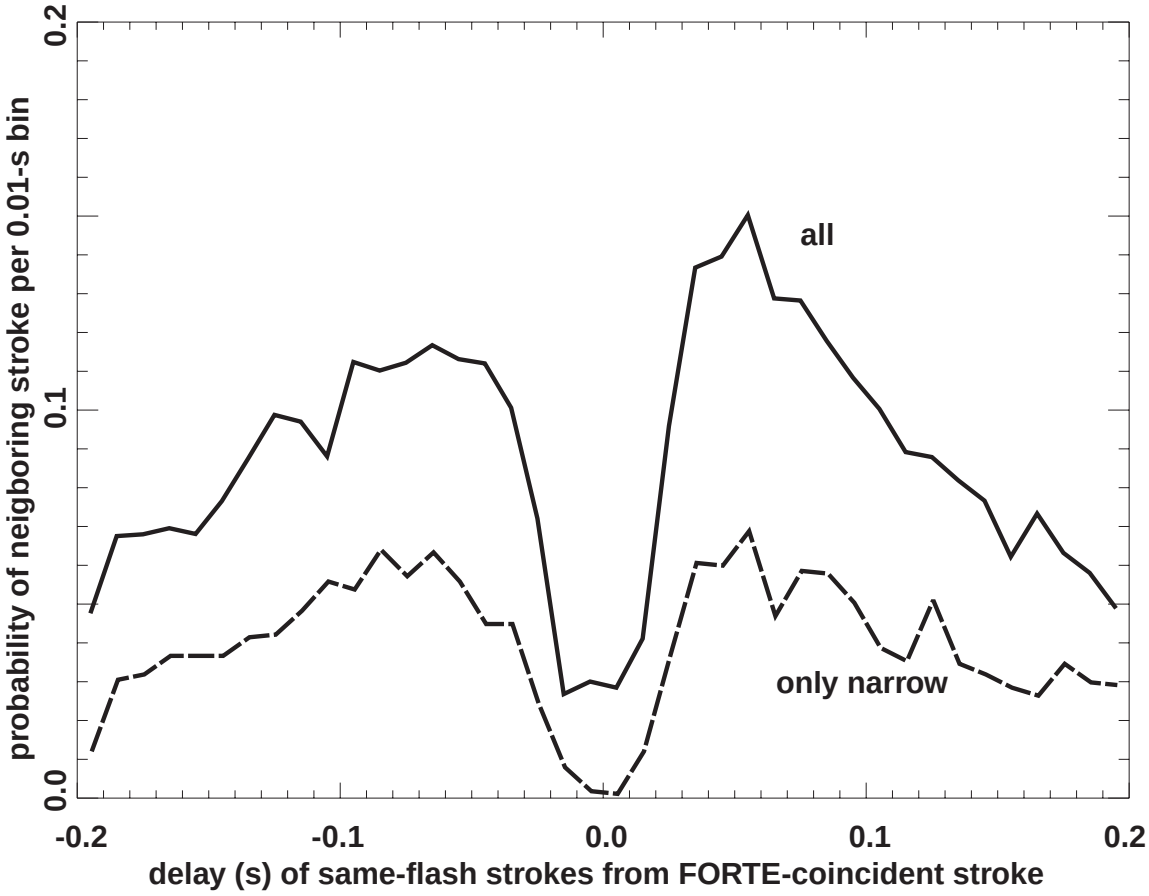

The FORTE observations of ~1400 narrow VHF pulses accompanying -CG strokes are marginally capable of indicating an intriguing satellite-elevation-angle dependence of their detection liklihood, relative to that of the parent distribution of ~10,000 VHF signals

accompanying -CG strokes. Figure 6 shows the satellite-elevation-angle distributions for both the parent distribution (dashed curve) and the narrow pulses (solid curve). Each distribution is separately normalized to have unity peak, so that their shapes can be readily compared. Apparently the narrow-pulse detection liklihood is marginally enhanced (relative to the background distribution of VHF signals accompanying -CG strokes) at intermediate elevation angles (20-35°). A follow-on paper will treat this exhaustively, incorporating both a realistic FORTE antenna model and an empirical FORTE triggering/detection model, and will thereby infer the *transmission pattern (versus elevation angle) of the VHF radiation process at the source*. That paper will also employ a more realistic event-selection process in order to correctly select narrow VHF pulses. Finally, that paper will treat the polarization of the VHF pulses exhaustively and will relate the polarization to the transmission pattern.

Figure 6: Observed distribution of FORTE elevation angles for detection of VHF signals that are closely coincident with NLDN strokes. The dashed curve is for all -CG strokes having FORTE coincidence. The solid curve is for the subset of these in which the coincident FORTE VHF pulse meets automatically applied criteria for extreme narrowness (<200 ns).

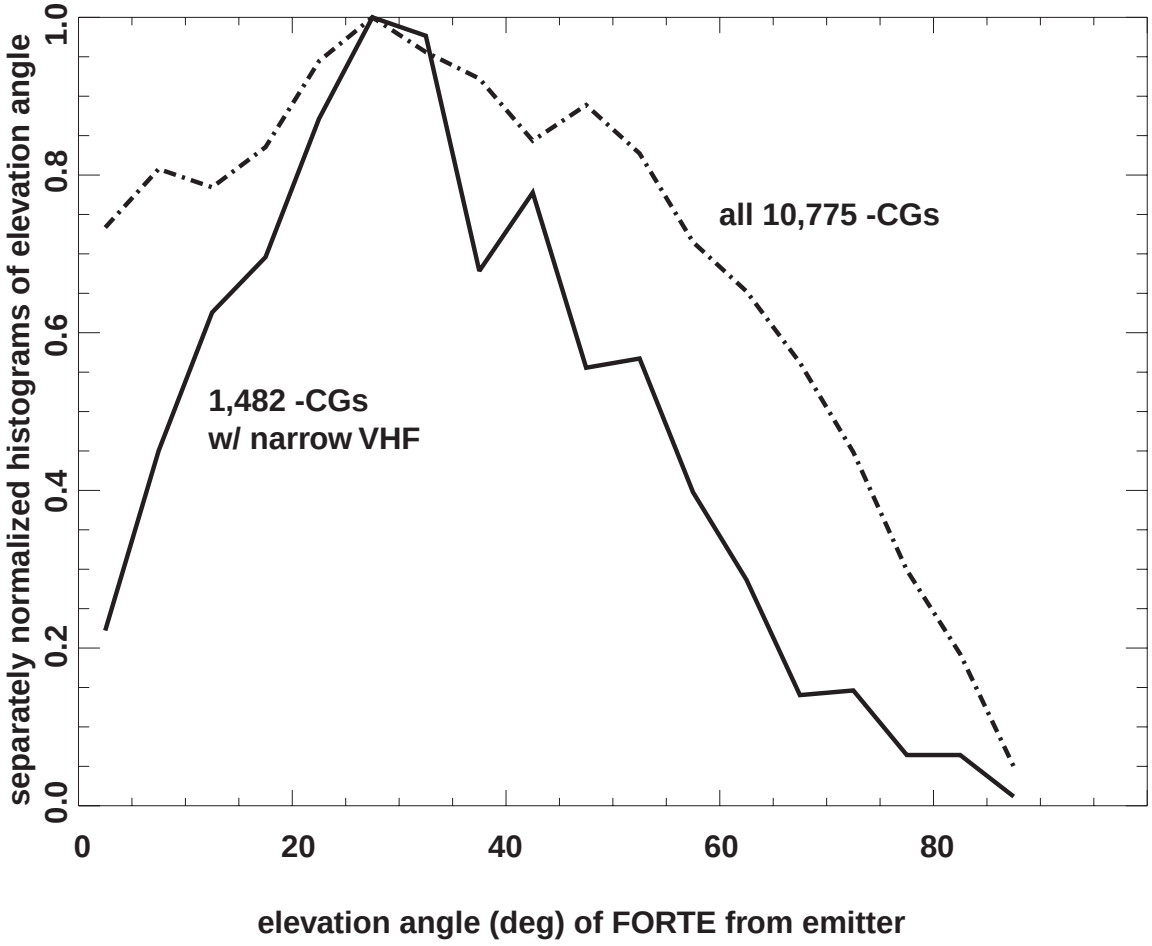

4. Discussion

4.1 Summary

The narrow pulses studied in this and the follow-on paper show several noteworthy properties. First, they are much more likely to be observed in association with -CG strokes than with either +CG strokes or IC strokes, when the stroke characterization can be made by NLDN coincidence. Second, the -CG strokes with which the narrow VHF pulses are associated are significantly more likely over sea than over land. Third, the VHF pulses usually appear to be linearly polarized. Fourth, the VHF pulses are as likely to accompany subsequent strokes, compared to first strokes, within -CG flashes of stroke multiplicity >1, although overall they are only half as likely to occur in such multi-sroke flashes, compared to the background distribution of all FORTE VHF events associated with -CG strokes. Fifth, the likelihood of FORTE triggering on a narrow VHF pulse accompanying -CG stroke initiation is enhanced at moderate elevation angles (20-35°), relative to the background distribution of all FORTE VHF events associated with -CG strokes.

4.2 Affinity for seawater, relative to dry-land location

The affinity of FORTE-observed narrow VHF pulses to occur over seawater suggests a meaning that is less ambiguous in the case of satellite observations than in the case of

ground-based observations. As reviewed in Section 1, the latter had to take pains to ensure salt-water propagation paths, in order to avoid selectively attenuating the higher frequencies during the signal transport from the lightning to the sensor. The FORTE observations involve an obliquely upward propagation path, so that the signal is expected to suffer much less lossy-groundplane distortion. Thus, the tendency of FORTE-observed narrow VHF pulses to occur over seawater tends to implicate the high-conductivity substrate afforded by seawater as influencing the timescale of the radiation process itself. This would not be surprising if the transient turn-on of the return-stroke current were regulated by a resistive/capacitive (RC) charging time involving the flow of ground currents to the vertical discharge through a resistive groundplane. It is useful to repeat that Heidler and Hopf [1998] noted that their data could not be explained by propagation effects alone, and that they inferred some *pulse-broadening at the source* of -CG strokes on land compared to those reported earlier by other authors over seawater. See also the comment on this by Willet *et al* [1998].

4.3 Polarization of signal

We repeat that the linear polarization of the narrow VHF pulses associated with -CG stroke initiation separates them from the majority of VHF signals emitted by lightning processes. The air-breakdown process [see in particular *Bondiou et al.*, 1990; *Renardieres*, 1981] is likely to produce incoherent, randomly polarized net radiation due

to the multiplicity of elementary radiators whose radiation overlaps in time at the receiver. By contrast, a single macroscopic radiating dipole is capable of radiating a linearly polarized signal. This is consistent with what FORTE sees in the case of narrow VHF pulses associated with -CG stroke initiation. It is also consistent with the broadband observations of Willett and others (see Section 1). The follow-on paper will discuss the evidence of the narrow pulses' implied emission pattern in terms of alternate models of a vertical current stalk whose time-varying current causes the radiation.

4.4 Amplitude of FORTE-observed narrow VHF pulses

As just mentioned, the data on narrow VHF pulses observed by FORTE appear to be consistent with the picture implied by the ground-based observations of Willett and others: That a rather simple radiated pulse, from a single dipole near the ground, is responsible for the entire radiation phenomenon, whether seen in the LF/VLF ("sferic") or the HF/VHF. We can further test the FORTE data for consistency with this picture by checking the amplitude of the radiated pulse as observed by FORTE within the passband 26-48 MHz. The spectra developed by Willett *et al* [1990] indicate that the spectral density is monotonically decreasing versus frequency througout the high HF range. Their passband extends as high as 30 MHz (the HF/VHF boundary), while the passband of FORTE in the present study is slightly higher in frequency (26-48 MHz) and only 2/3 as wide. Therefore, if the range-corrected pulse amplitude in the FORTE passband, after

dechirping as well as we can, exceeded the range-corrected pulse amplitude in the time-domain waveforms discussed elsewhere by Willett *et al* [1998] and Willett and Krider [*Willett and Krider*, 2000], we would have a troubling inconsistency between the FORTE and the ground-based observations. We check on this as follows: Willett and Krider [*Willett and Krider*, 2000, Figure 5] show peak transient electric field amplitudes in the fast pulse, scaled to 100-km distance, in the range of 2-5 V/m. With FORTE observations we typically see a peak field amplitude of 1-5 mV/m (see, for example, Figures 1 and 2 above) at typical ranges of 1500 km. Scaling the amplitude linearly with inverse distance, the FORTE-observed amplitudes in a 22-MHz bandwidth scaled to 100-km distance, are in the range 0.015-0.045 V/m. These are approximately 100-fold weaker than the pulses seen on the ground by Willett and Krider.

On the other hand, the spectral estimates by Willett *et al* [1990, e.g. their Figures 3 and A6] suggest that in the range 10-20 MHz, the signal spectral density rolls off versus frequency as PSD ~ f^{-10}, and thus that the electric field amplitude varies as E ~ f^{-5}. Given that the FORTE passband (26-48 MHz) is only a factor of ~2 higher than the passband (0-30 MHz) in which Willett and Krider's [2000] waveforms were recorded, we expect their distance-scaled field amplitude to exceed FORTE's by a factor on the order of 2^5, or 32. That the roughly estimated ratio of 100 (see above) is so close to the ratio implied by the spectral slopes in Willett *et al* [1990] lends credence to the idea that the radiation

phenomenon is the same for both the ground-based and the FORTE observations, notwithstanding their slightly different passbands. The distribution of pulse amplitudes in the FORTE data will be exhaustively treated in the follow-up publication.

Acknowledgements

We wish to acknowledge useful conversations with Dr. John Willett, Dr. Anne Bondiou-Clergerie, Dr. Kenneth Cummins, Dr. Paul Krehbiel, Dr. Martin Murphy, and Dr. Earle Williams. We are indebted to the FORTE operations team, led by Phil Klingner and Diane Roussel-Dupré, for constant support in acquiring and working with FORTE data. The work described here was performed under the auspices of the United States Department of Energy.

References

Bondiou, A., I. Taudiere, P. Richard, and F. Helloco, Analyse spatio-temporelle du rayonnement VHF-UHF associe a l'eclair, *Revue Phys. Appl.*, *25*, 147-157, 1990.

Cooray, V., and S. Lundquist, Characteristics of the radiation fields from lightning in Sri Lanka in the tropics, *J. Geophys. Res.*, *90* (D4), 6099-6109, 1985.

Cooray, V., and Y. Ming, Propagation effects on the lightning-generated electromagnetic fields for homogeneous and mixed land-sea paths, *J. Geophys. Res.*, *99* (D5), 10,641-10,652, 1994.

Cummins, K.L., M.J. Murphy, E.A. Bardo, W.L. Hiscox, R. Pyle, and A.E. Pifer, Combined TOA/MDF technology upgrade of U. S. National Lightning Detection Network, *J. Geophys. Res.*, *103* (D8), 9035-9044, 1998.

Heidler, F., and C. Hopf, Measurement results of the electric fields in cloud-to-ground lightning in nearby Munich, Germany, *IEEE Trans. Electromag. Compat.*, *40* (4), 436-443, 1998.

Holden, D.N., C.P. Munson, and J.C. Devenport, Satellite observations of transionospheric pulse pairs, *Geophys. Res. Lett.*, *22* (8), 889-892, 1995.

Idone, V.P., D.A. Davis, P.K. Moore, Y. Wang, R.W. Henderson, M. Ries, and P.F. Jamason, Performance evaluation of the U. S. National Lightning Detection Network in eastern New York 1. Detection efficiency, *J. Geophys. Res.*, *103* (D8), 9045-9055, 1998a.

Idone, V.P., D.A. Davis, P.K. Moore, Y. Wang, R.W. Henderson, M. Ries, and P.F. Jamason, Performance evaluation of the U. S. National Lightning Detection Network in eastern New York 2. Location accuracy, *J. Geophys. Res.*, *103* (D8), 9057-9069, 1998b.

Jacobson, A.R., K.L. Cummins, M. Carter, P. Klingner, D. Roussel-Dupré, and S.O. Knox, FORTE radio-frequency observations of lightning strokes detected by the National Lightning Detection Network, *J. Geophys. Res.*, *105* (D12), 15,653, 2000.

Jacobson, A.R., S.O. Knox, R. Franz, and D.C. Enemark, FORTE observations of lightning radio-frequency signatures: Capabilities and basic results, *Radio Sci.*, *34* (2), 337-354, 1999.

Jacobson, A.R., and X.-M. Shao, Using geomagnetic birefringence to locate sources of impulsive, terrestrial VHF signals detected by satellites on orbit, *Radio Sci.*, *36* (4), 671-680, 2001.

Krider, E.P., and C. Leteinturier, Submicrosecond fields radiated during the onset of first return strokes in cloud-to-ground lightning, *J. Geophys. Res.*, *101* (D1), 1589-1597, 1996.

Krider, E.P., G.J. Radda, and R.C. Noggle, Regular radiation field pulses produced by intracloud lightning discharges, *J. Geophys. Res.*, *80* (27), 3801-3804, 1975.

Le Vine, D.M., Sources of the strongest RF radiation from lightning, *J. Geophys. Res.*, *85* (C7), 4091-4095, 1980.

Leteinturier, C., J. Hamelin, and A. Eybert-Berard, Submicrosecond characteristics of lightning return-stroke currents, *IEEE Trans. Electromag. Compat.*, *33* (4), 351-357, 1991.

LeVine, D.M., J.C. Willett, and J.C. Bailey, Comparison of fast electric field changes from subsequent return strokes of natural and triggered lightning, *J. Geophys. Res.*, *94* (D11), 13,259-13,265, 1989.

Light, T.E., D.M. Suszcynsky, and A.R. Jacobson, Coincident Radio Frequency and Optical Emissions from Lightning, Observed with the FORTE Satellite, *J. Geophys. Res.*, *accepted*, 2001.

Massey, R.S., and D.N. Holden, Phenomenology of transionospheric pulse pairs, *Radio Sci., 30* (5), 1645-1659, 1995.

Massey, R.S., D.N. Holden, and X.-M. Shao, Phenomenology of trans-ionospheric pulse pairs: Further observations, *Radio Sci, 33*, 1755-1761, 1998a.

Massey, R.S., S.O. Knox, R.C. Franz, D.N. Holden, and C.T. Rhodes, Measurements of transionospheric radio propagation parameters using the FORTE satellite, *Radio Sci., 33* (6), 1739-1753, 1998b.

Mazur, V., L.H. Ruhnke, A. Bondiou-Clergerie, and P. Lalande, Computer simulation of a downward negative stepped leader and its interaction with a ground structure, *J. Geophys. Res., 105* (D17), 22,361-22,369, 2000.

Proctor, D.E., VHF radio pictures of cloud flashes, *J. Geophys. Res., 86* (C5), 4041-4071, 1981.

Renardieres, G.d., L'amorcage en polarite negative des grands intervalles d'air aux Renardieres- Resultats de 1978 (Negative discharges in long air gaps at les Renardieres-1978 results), *Electra*, *74*, 68-216, 1981.

Shao, X.-M., and A.R. Jacobson, Polarization observations of broadband VHF signals by the FORTE satellite, *Radio Science*, *submitted*, 2001.

Shao, X.M., P.R. Krehbiel, R.J. Thomas, and W. Rison, Radio interferometric observations of cloud-to-ground lightning phenomena in Florida, *J. Geophys. Res.*, *100* (D2), 2,749-2,783, 1995.

Smith, D.A., X.M. Shao, D.N. Holden, C.T. Rhodes, M. Brook, P.R. Krehbiel, M. Stanley, W. Rison, and R.J. Thomas, Distinct, isolated thunderstorm radio emissions, *J. Geophys. Res.*, *104*, 4189-4212, 1998.

Taylor, W.L., E.A. Brandes, W.D. Rust, and D.R. MacGorman, Lightning activity and severe storm structure, *Geophys. Res. Lett.*, *11* (5), 545-548, 1984.

Uman, M.A., V.A. Rakov, K.J. Schnetzer, K.J. Rambo, D.E. Crawford, and R.J. Fisher, Time derivative of the electric field 10, 14, and 30 m from triggered lightning strokes, *J. Geophys. Res., 105* (D12), 15,577-15,595, 2000.

Weidman, C.D., and E.P. Krider, Submicrosecond risetimes in lightning return-stroke fields, *Geophys. Res. Lett., 7* (11), 955-958, 1980.

Willett, J.C., J.C. Bailey, and E.P. Krider, A class of unusual lightning electric field waveforms with very strong high-frequency radiation, *J. Geophys. Res., 94* (D13), 16255-16267, 1989.

Willett, J.C., J.C. Bailey, C. Leteinturier, and E.P. Krider, Lightning electromagnetic radiation field spectra in the interval from 0.2 to 20 MHz, *J. Geophys. Res., 95* (D12), 20,367-20,387, 1990.

Willett, J.C., and E.P. Krider, Rise times of impulsive high-current processes in cloud-to-ground lightning, *IEEE Trans. Ant. Prop., 48* (9), 1442-1451, 2000.

Willett, J.C., E.P. Krider, and C. Leteinturier, Submicrosecond field variations during the onset of first return strokes in cloud-to-ground lightning, *J. Geophys. Res.*, *103* (D8), 9027-9034, 1998.